Increased Dynamic Effects in a Catalytically Compromised Variant of *Escherichia coli* Dihydrofolate Reductase

J. Javier Ruiz-Pernia,[†,∥] Louis Y. P. Luk,[‡,∥] Rafael García-Meseguer,[§] Sergio Martí,[†] E. Joel Loveridge,[‡]
Iñaki Tuñón,*[§] Vicent Moliner,*[†] and Rudolf K. Allemann*[‡]

[†]Departament de Química Física i Analítica, Universitat Jaume I, 12071 Castello, Spain

[‡]School of Chemistry & Cardiff Catalysis Institute, Cardiff University, Park Place, Cardiff, CF10 3AT, U.K.

[§]Departament de Química Física, Universitat de València, 46100 Burjassot, Spain

Ⓢ *Supporting Information*

A dynamic 'knock-in'
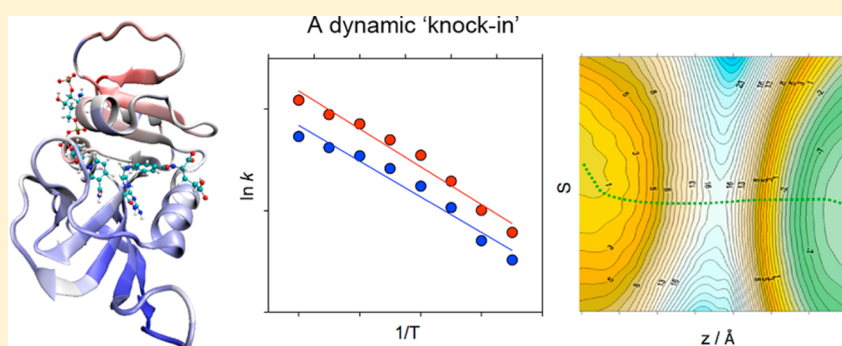
ABSTRACT: Isotopic substitution (^{15}N, ^{13}C, ^{2}H) of a catalytically compromised variant of *Escherichia coli* dihydrofolate reductase, EcDHFR-N23PP/S148A, has been used to investigate the effect of these mutations on catalysis. The reduction of the rate constant of the chemical step in the EcDHFR-N23PP/S148A catalyzed reaction is essentially a consequence of an increase of the quasi-classical free energy barrier and to a minor extent of an increased number of recrossing trajectories on the transition state dividing surface. Since the variant enzyme is less well set up to catalyze the reaction, a higher degree of active site reorganization is needed to reach the TS. Although millisecond active site motions are lost in the variant, there is greater flexibility on the femtosecond time scale. The "dynamic knockout" EcDHFR-N23PP/S148A is therefore a "dynamic knock-in" at the level of the chemical step, and the increased dynamic coupling to the chemical coordinate is in fact detrimental to catalysis. This finding is most likely applicable not just to hydrogen transfer in EcDHFR but also to other enzymatic systems.

INTRODUCTION

The involvement of protein motions in the chemical step of enzyme reactions that involve hydrogen (H^+, $H^•$, or H^-) tunnelling remains one of the most discussed topics in modern enzymology. Early computational evidence suggested that dynamic effects may not be required to account for enzymatic catalysis and that the participation of protein motions in the chemical step can be satisfactorily described as equilibrium fluctuations.[1] Nevertheless, theoretical frameworks that involve protein "promoting vibrations" or "promoting motions" on femtosecond to millisecond time scales, which are proposed to reduce the height and/or width of the potential energy barrier and thereby enhance enzymatic catalysis,[2−4] have been invoked to interpret experimental data.[5−11] Protein motions occur over a hierarchy of time scales and ranges,[12,13] from femtosecond local bond vibrations to millisecond large scale domain motions. It has been suggested that motions on one time scale may facilitate motions on another.[14,15] A number of theoretical analyses based on atomistic simulations have suggested that protein motions may not significantly contribute

to reducing the free energy barrier of enzyme catalyzed reactions,[16−20] and several experimental studies have shown that models which require a contribution from protein motions for catalysis do not seem fully compatible with the available data.[21−28] A combination of experimental results, QM/MM simulations, and theoretical analyses has however recently revealed that the dynamics of the protein environment do have a small but measurable effect on the chemical reaction.[28]

Dihydrofolate reductase (DHFR) has often been used in studies of the relationship between protein motions and catalysis.[5−7,29−33] It catalyzes the NADPH-dependent reduction of 7,8-dihydrofolate (H_2F) to 5,6,7,8-tetrahydrofolate (H_4F) by hydride transfer from C4 of NADPH and protonation of N5 of H_2F (Figure 1). The catalytic cycle of DHFR from *E. coli* (EcDHFR) has been thoroughly characterized;[33−35] the physical steps of substrate binding and product release involve large scale millisecond time scale
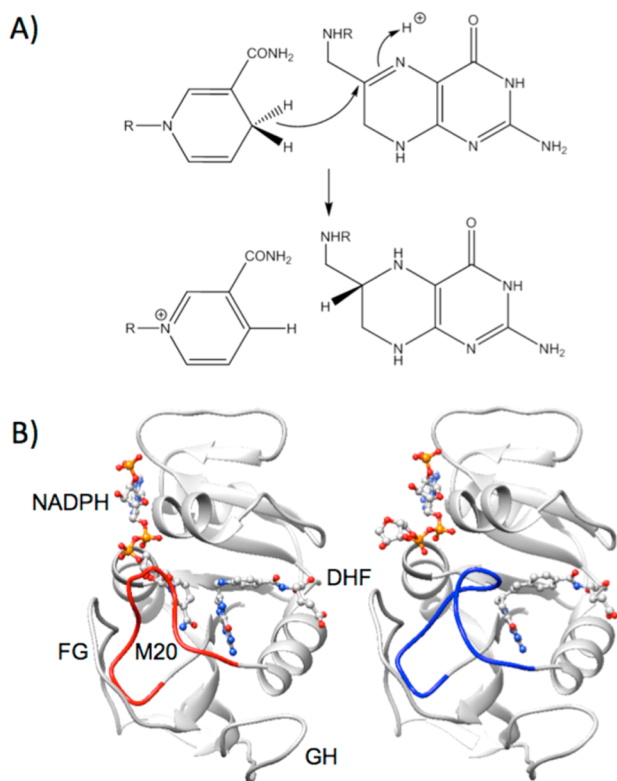
Figure 1. (A) Conversion of dihydrofolate to tetrahydrofolate through transfer of the pro-R hydride of NADPH and a solvent proton. (B) Cartoon representation of the closed and occluded conformations of EcDHFR. Catalytically important loops (M20, βFG, and GH), substrate (H_2F), and cofactor (NADPH) are labeled. The M20 loop is highlighted in red in the closed conformation and in blue in the occluded conformation. The cofactor and substrate are represented using ball-and-stick models.

conformational motions of the M20 loop (residues 9−24), which forms part of the active site.[33,34] The closed conformation, found in the holo-enzyme and the Michaelis complex,[34] is stabilized by hydrogen bonding from the M20 loop to the neighboring βFG loop (residues 116−132). Following hydride transfer, the M20 loop adopts the occluded conformation, which is stabilized by hydrogen bonds from the M20 loop to the neighboring βGH loop (residues 142−149). This prevents the nicotinamide ring of the cofactor NADP(H) from entering the active site[34] (Figure 1).

A recent report of a "dynamic knockout" of EcDHFR has reignited controversy over the role of protein motions in hydrogen transfer reactions.[36] EcDHFR-N23PP/S148A is unable to adopt the occluded conformation due to the absence of the crucial hydrogen bonds between the M20 and βGH loops, and millisecond to microsecond time scale motions observed in the M20 loop of wild type EcDHFR are lost in the variant.[36] This "dynamic knockout" displayed reduced hydride transfer rate constants, and it was proposed that the protein motions lost in EcDHFR-N23PP/S148A are involved in promoting hydride transfer in wild type EcDHFR.[36] However, theoretical studies based on the empirical valence bond approach suggested that the reduction in the hydride transfer rate constant in EcDHFR-N23PP/S148A was due to effects on the electrostatic preorganization and consequently the reorganization free energy within the active site.[37] Measurement of the kinetic isotope effects of the EcDHFR-N23PP/S148A

catalyzed hydride transfer reaction provided further evidence that the loss of protein motions may not be the cause of the impaired catalysis.[27] A number of other studies have also suggested that protein motions do not promote the chemical step in wild type EcDHFR catalysis,[16,24−26,31,38] but the issue continues to generate debate in the literature.

The Born−Oppenheimer approximation assumes that, while isotopic substitutions do not affect the electronic potential energy surface, mass-dependent differences result in changes in atomic motions from femtosecond bond vibrations to millisecond time scale conformational changes.[39] Hence, enzymatic isotopic substitution to form "Born−Oppenheimer enzymes"[40,41] has been postulated to affect catalysis by changing protein motions that couple to the reaction coordinate.[40−43] Accordingly, we have recently shown by a combination of experimental and computational studies of light (natural isotopic abundance) and heavy (^{15}N, ^{13}C, ^{2}H isotopically substituted) EcDHFR that mass-dependent protein motions in EcDHFR affect the dynamic recrossing of hydride transfer but they do not promote tunnelling, and that the increased number of recrossing trajectories has a slight effect on the effective barrier of the chemical step.[28]

The present investigation analyzes the dynamic contributions to enzyme catalysis by comparing heavy EcDHFR-N23PP/S148A with its light counterpart. In particular, we report experimental and computational results that allow characterization of the dynamics of the coordinates associated with the hydride transfer from NADPH to H_2F. We provide strong evidence that the loss of protein motions observed previously by NMR[36] does not directly impact catalysis of the hydride transfer step; in fact, the chemical step is subject to *greater* dynamic contributions in the "dynamic knockout" than in the wild type enzyme. Together with the increased reaction barrier, the increased dynamic coupling to the chemical coordinate is the cause of the reduction of the hydride transfer rate observed in EcDHFR-N23PP/S148A.

■ RESULTS AND DISCUSSION

Creation of "Heavy" EcDHFR-N23PP/S148A. "Heavy" EcDHFR-N23PP/S148A was produced in M9 medium containing exclusively $^{15}NH_4Cl$, U−^{13}C,^{2}H-glucose, and $^{2}H_2O$. After purification in buffers made of $^{1}H_2O$, heavy EcDHFR-N23PP/S148A showed a 10.02% increase in molecular mass (Figures S1 and S2, Supporting Information), indicating that 91.2% of the ^{14}N, ^{12}C, and non-exchangeable ^{1}H atoms had been replaced by their heavier isotopes. The secondary structures of light and heavy EcDHFR-N23PP/S148A were indistinguishable as measured by circular dichroism spectroscopy (Figure S3, Supporting Information).

Experimental Results. The nature of the rate limiting step in DHFR catalysis is dependent on pH.[35] At pH 7, the release of NADP$^+$ from the binary EcDHFR-N23PP/S148A·NADP$^+$ complex is most likely rate limiting,[36] whereas the release of H_4F from the E·NADPH·H_4F mixed ternary complex is rate limiting in wild type EcDHFR.[35] Neither the Michaelis constants K_M nor the turnover numbers k_{cat} were sensitive to isotopic substitution of EcDHFR-N23PP/S148A (Tables S2 and S3, Supporting Information). In the EcDHFR·NADP$^+$ complex as well as in the apoenzyme, the loop regions are largely disordered[44] and hence NADP$^+$ release is unlikely to involve a significant conformational change in either the wild type or variant enzyme. In contrast, a significant enzyme KIE_{cat} ($k_{cat}^{LE}/k_{cat}^{HE}$, where LE and HE indicate light and heavy
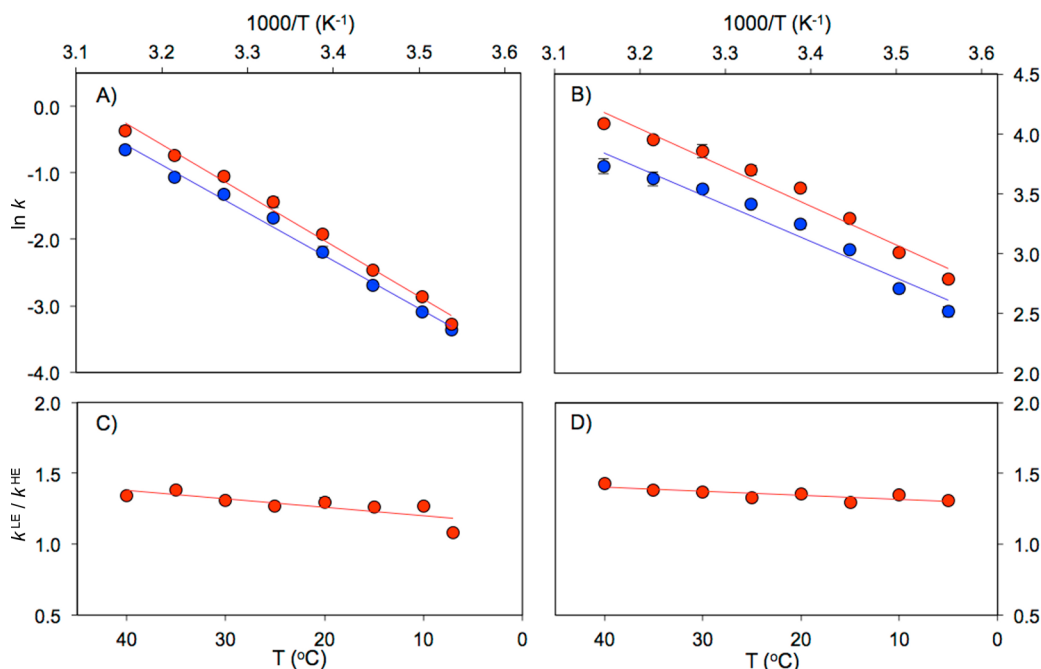
Figure 2. Temperature dependence of the experimental EcDHFR-N23PP/S148A hydride transfer rate constants. (A) pH 9.5 steady state kinetic data; (B) pH 7.0 pre-steady-state kinetic data. Data and Arrhenius fits are shown in red for the light enzyme and in blue for the heavy enzyme. (C and D) The enzyme KIE (ratio of light to heavy enzyme rate constants, k^{LE}/k^{HE}) at pH 9.5 and pH 7.0, respectively.

Table 1. Experimentally Determined Rate Constants and Enzyme KIEs for Hydride Transfer in Light and Heavy EcDHFR-N23PP/S148A at 25 °C and Activation Parameters from Fitting the Experimental Data to the Arrhenius Equation[a]

enzyme and pH	k (s^{-1})	enzyme KIE	E_a (kJ·mol^{-1})	ΔE_a (kJ·mol^{-1})	A_H (s^{-1})	A_H^{LE}/A_H^{HE}
light EcDHFR, pH 7	178.2 ± 4.7	1.10 ± 0.03	31.84 ± 0.69	5.78 ± 1.61	(6.42 ± 0.81) × 10^7	10.74 ± 0.13
heavy EcDHFR, pH 7	151.6 ± 4.2		26.05 ± 1.45		(5.98 ± 0.11) × 10^6	
light EcDHFR, pH 9.5	1.86 ± 0.18	1.13 ± 0.08	60.65 ± 0.72	3.15 ± 1.28	(7.49 ± 0.31) × 10^{10}	4.09 ± 0.24
heavy EcDHFR, pH 9.5	1.64 ± 0.16		57.50 ± 1.06		(1.83 ± 0.43) × 10^{10}	
light EcDHFR-N23PP/S148A, pH 7	40.32 ± 0.79	1.33 ± 0.02	27.14 ± 0.16	1.52 ± 0.31	(2.17 ± 0.14) × 10^6	2.50 ± 0.11
heavy EcDHFR-N23PP/S148A, pH 7	30.41 ± 0.80		25.62 ± 0.27		(8.63 ± 0.75) × 10^5	
light EcDHFR-N23PP/S148A, pH 9.5	0.24 ± 0.01	1.27 ± 0.03	63.98 ± 0.01	3.57 ± 0.79	(3.54 ± 0.51) × 10^{10}	5.44 ± 0.19
heavy EcDHFR-N23PP/S148A, pH 9.5	0.19 ± 0.01		60.41 ± 0.79		(6.51 ± 0.83) × 10^9	

[a]Data for light and heavy wild type EcDHFR are from ref 28.

enzyme, respectively) on the steady-state rate constants for wild type EcDHFR of 1.16 ± 0.01 at 35 °C was observed,[28] consistent with the large conformational change observed on H$_4$F release.[33,34]

For pH values above 9, hydride transfer from NADPH to H$_2$F determines k_{cat}.[27,35,36] The steady-state rate constants measured at pH 9.5 for light and heavy EcDHFR-N23PP/S148A showed a temperature dependent enzyme KIE$_{cat}$, such that k_{cat}^{LE} is 14% larger than k_{cat}^{HE} at 10 °C and 34% larger at 40 °C (Figure 2, Tables S1 and S2, Supporting Information). The enzyme KIE was higher in EcDHFR-N23PP/S148A than in wild type EcDHFR at all temperatures. In contrast, the Michaelis constants for NADPH and for H$_2$F are unaffected by isotopic substitution at both 20 and 35 °C (Table S3, Supporting Information), indicating that binding interactions are unchanged in the heavy enzyme and therefore that, at pH 9.5, the enzyme KIE reflects a difference in reactivity between the light and heavy enzymes after the formation of the respective Michaelis complexes.

Hydride transfer at pH 9.5 is not physiologically significant,[25] so the rate constants of the fast hydride transfer from reduced NADPH to mostly protonated H$_2$F were determined at pH 7.0

in pre-steady-state stopped-flow experiments, in which the fluorescence resonance energy transfer from the protein to reduced NADPH was measured. The pH dependence of the pre-steady-state hydride transfer rate constants indicated that the apparent pK_a of the EcDHFR-N23PP/S148A catalyzed reaction was not affected by isotopic substitution (Figure S4 and Table S4, Supporting Information). The apparent pK_a values for the reactions catalyzed by light and heavy EcDHFR-N23PP/S148A were 6.29 ± 0.10 and 6.23 ± 0.09 at 20 °C and 6.35 ± 0.16 and 6.15 ± 0.05 at 35 °C. The hydride transfer rate constants for light and heavy EcDHFR-N23PP/S148A (k_H^{LE} and k_H^{HE}) at pH 7.0 show a similar dependence on temperature to that observed in the steady state measurements at elevated pH (Table S1, Supporting Information; Figure 2). The enzyme KIE$_H$ (k_H^{LE}/k_H^{HE}) increased from 1.31 ± 0.03 at 10 °C to 1.43 ± 0.04 at 40 °C (Figure 2). These are significantly higher than the corresponding values of 0.93 ± 0.02 at 10 °C to 1.18 ± 0.09 at 40 °C reported previously for the reaction catalyzed by wild type EcDHFR.[28] Activation energies were slightly higher in light EcDHFR-N23PP/S148A than in the heavy counterpart, with the reduction in free energy for the reaction resulting from lower Arrhenius prefactors and hence a less favorable activation

Table 2. Results from the QM/MM Simulations for Hydride Transfer in Light and Heavy EcDHFR-N23PP/S148A[a]

enzyme	γ	κ	ΔG_{act}^{QC} (kcal·mol^{-1})	ΔG_{eff} (kcal·mol^{-1})	k_{theor} (s^{-1})	$(k^{LE}/k^{HE})_{theor}$	k_H (s^{-1})	$(k^{LE}/k^{HE})_{exp}$
light EcDHFR-N23PP/S148A	0.53 ± 0.02	2.25 ± 0.45	16.43 ± 0.70	16.63 ± 0.84	8.0	1.26 ± 0.04	47.23 ± 1.28	1.37 ± 0.03
heavy EcDHFR-N23PP/S148A	0.42 ± 0.02			16.74 ± 0.84	6.3		34.44 ± 1.18	
light EcDHFR	0.57 ± 0.02	2.61 ± 0.49	14.59 ± 0.41	14.35 ± 0.54	219	1.16 ± 0.04	209.1 ± 5.0	1.10 ± 0.04
heavy EcDHFR	0.49 ± 0.02			14.46 ± 0.54	188		190.1 ± 8.5	

[a]Transmission coefficient components due to recrossing (γ) and tunnelling (κ), quasi-classical (QC) free energy of activation (ΔG_{act}^{QC}) (eq 1), effective phenomenological free energies of activation (ΔG_{eff}), and predicted (k_{theor}, at 300 K) and experimental (k_H, at 303 K) hydride transfer rate constants are included. 200 trajectories were obtained to give these data. Components of the quasi-classical activation free energy, the potential of mean force (PMF) difference between the TS and the reactants, and the classical and quantized vibration corrections are reported in the Supporting Information. Data for light and heavy wild type EcDHFR are from ref 28.

entropy (Table 1). The same situation had also been observed in the reaction catalyzed by wild type EcDHFR.[28] The reduced rate constants for hydride transfer in EcDHFR-N23PP/S148A relative to EcDHFR have also been shown to be the result of less favorable activation entropy in the variant, rather than increased activation enthalpies.[27]

Molecular Dynamics Simulations—Enzyme Isotope Effects. Our analysis of the rate constant of the chemical step is based on transition state theory (TST), modified to account for tunnelling contributions and other dynamic effects:[45−47]

$$k(T) = \Gamma(T,z)\frac{k_B T}{h} \exp\left(-\frac{\Delta G_{act}^{QC}(T,z)}{RT}\right) \qquad (1)$$

where R is the ideal gas constant, T is the temperature, k_B is the Boltzmann constant, h is Planck's constant, $\Delta G_{act}^{QC}(T,z)$ is the quasi-classical activation free energy[48] (for details, see the Supporting Information) obtained as a function of a reaction coordinate z that corresponds to the transfer of the hydride from the donor atom of the cofactor to the substrate's acceptor atom ($z = d(C4_{NADPH}-H_t) - d(C6_{H2F}-H_t)$), and $\Gamma(T,z)$ is the temperature-dependent transmission coefficient, which contains the dynamic corrections to the classical rate constant and is therefore equal to unity in the limit of classical TST. Although different contributions are in principle coupled, $\Gamma(T,z)$ can be expressed as

$$\Gamma(T,z) = \gamma(T,z)\cdot\kappa(T) \qquad (2)$$

where $\gamma(T,z)$ is the recrossing transmission coefficient that corrects the rate constant for trajectories that recross the dividing surface back to the reactant valley and $\kappa(T)$ is the tunnelling coefficient that accounts for reactive trajectories that do not reach the classical threshold energy. Because the definition of the selected reaction coordinate (z) involves only coordinates of atoms from the reacting subsystem (substrate and cofactor), the dynamic impact of protein motions in the chemical step will be reflected in a recrossing coefficient that deviates from unity. The two terms of eq 2 can be obtained from QM/MM simulations (for details, see the Supporting Information). The same approach has previously been used to analyze the reactivity of wild type EcDHFR.[28]

The calculated rate constants for wild type EcDHFR (Table 2) are in excellent agreement with the experimental data,[28] while the values calculated for EcDHFR-N23PP/S148A are somewhat smaller than those measured by experiment. This is most probably due to a small systematic error in the energy function that leads to an overestimation of the free energy barrier. However, the difference is below 1 kcal·mol^{-1} and of

the same order of magnitude as the statistical uncertainty associated with the free energies (Table 2). The calculations show clearly that the reduction in the rate constant in EcDHFR-N23PP/S148A relative to the wild type enzyme is essentially due to the increase in the quasi-classical activation free energy (Table 2), while the recrossing transmission coefficients are similar but distinct and tunnelling contributions are also very close in both wild type and variant enzyme (Table 2). These results support the previous conclusions that the reduction in the rate constant in EcDHFR-N23PP/S148A is not due to the impact of a "dynamic knockout" on the chemical step but to a change in the properties of the equilibrium in the reactant state (RS) and transition state (TS) ensembles.[27,37] As discussed below, mutations provoke subtle changes in average protein−protein and protein−substrate/cofactor interactions that affect the free energy barrier.

Comparison of heavy and light EcDHFR and EcDHFR-N23PP/S148A shows that the difference in phenomenological rate constants between isotopomers arises from differences in the recrossing coefficients (γ). Tunnelling contributions (κ) are not affected by the change in mass between the light and heavy enzymes, which is not in agreement with proposals of tunnelling enhancement by dynamic coupling.[2−4] According to our simulations, such compressive "promoting" motions need not be invoked to explain the observed changes in reactivity; this finding is in agreement with recent work that revealed that "promoting vibrations" do not drive hydride transfer in the active site of EcDHFR.[38] However, the value of the recrossing transmission coefficient (γ) reflects the subtle coupling of protein environmental motions to the reaction coordinate in a way that is only apparent via a global description of all atomic positions. When the mass of the enzyme is increased, these motions are slower and the chemical system is not so efficient in relaxing to the reactant or product valleys after crossing the TS. This leads to an increase in the number of recrossings and therefore a reduction of the value of γ in the heavy enzyme relative to its light counterpart.

Simulations successfully reproduce the larger enzyme isotope effects obtained experimentally for the variant (Table 2). The computed k^{LE}/k^{HE} values for the variant and wild type enzymes are 1.26 and 1.16, while the experimental values are 1.37 and 1.10. The increased enzyme KIE for EcDHFR-N23PP/S148A relative to the wild type provides strong support for enhanced coupling of protein environmental motions to the reaction coordinate in the variant so that the chemical step becomes more sensitive to global protein motions in the modified enzyme. Our results show that the dynamic impact of protein motions on the chemical step is in fact larger in EcDHFR-
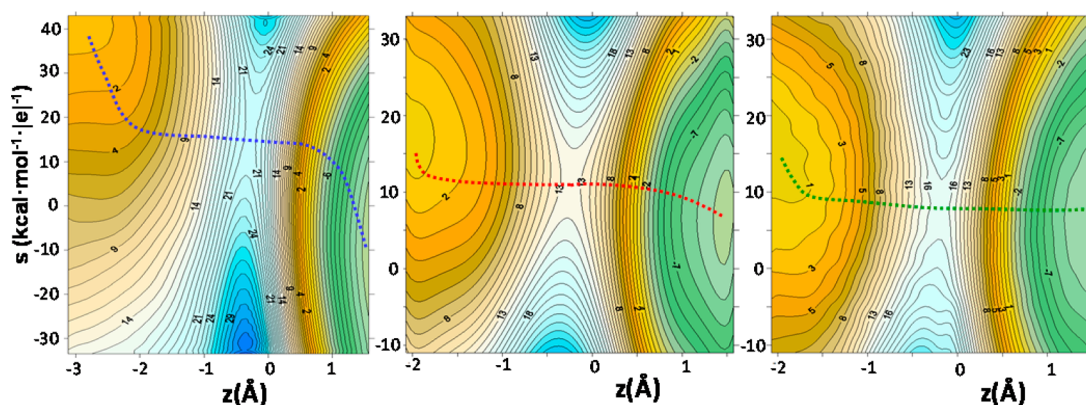
18692

dx.doi.org/10.1021/ja410519h | J. Am. Chem. Soc. 2013, 135, 18689−18696

Figure 3. Free energy surfaces corresponding to the hydride transfer from NADPH to protonated H$_2$F in aqueous solution (left), wild type EcDHFR (middle), and EcDHFR-N23PP/S148A (right). See text for a full description of the two coordinates. Each isoenergetic line represents a 1 kcal·mol^{-1} increase in free energy. The dotted lines represent the minimum free energy paths on the free energy surfaces obtained from the gradient of the surface.

N23PP/S148A than in the wild type enzyme, as reflected by the larger deviation from unity observed in the recrossing transmission coefficients of 0.53 and 0.42 for light and heavy EcDHFR-N23PP/S148A versus 0.57 and 0.49 for light and heavy EcDHFR. Further simulations were conducted to rationalize this unexpected behavior of the "dynamic knockout" variant.

Protein Motions in EcDHFR and EcDHFR-N23PP/S148A. To gain insight into the role of protein motions in EcDHFR and EcDHFR-N23PP/S148A, simulations of the free energy landscape of the enzymes were performed. Free energy surfaces (FESs) for hydride transfer in wild type EcDHFR and EcDHFR-N23PP/S148A and in the absence of an enzyme in aqueous solution were traced as a function of two coordinates (Figure 3; see the Supporting Information for details), namely, the solute (or chemical) coordinate (z) that corresponds to the transfer of the hydride and a solvent (or environmental) coordinate (s) that captures those environmental motions relevant for the chemical process.[49] This coordinate is obtained as the antisymmetric combination of the electrostatic potential created by the protein and aqueous environment on the donor and acceptor carbon atoms ($s = V(\text{C4}_{\text{NADPH}}) - V(\text{C6}_{\text{H2F}})$) and is analogous to the solvent polarization in Marcus theory of electron transfer reactions.[50]

A more complete description of the chemical process can be obtained by following the minimum free energy paths traced on the FESs (Figure 3). In all cases, the reaction starts with a change in the solvent coordinate, then essentially moves along the chemical coordinate to pass through the TS, and finishes with a new change in the solvent coordinate, leading to the relaxed products. Thus, the reaction proceeds with participation of the solvent coordinate, mostly before and after crossing the TS region. This explains the small deviation from unity observed in all the recrossing transmission coefficients reported in the previous section.

Environmental motions involved in the evolution from the Michaelis complex to the TS can be characterized by means of the frequency associated with the solvent coordinate. To this end, the force constants were evaluated from a parabolic fit of the free energy landscape along the solvent coordinate and the associated effective masses were derived from the equipartition theorem. From these data, the resulting frequencies for the three environments can be calculated. The values of the force constants found for the enzymes (2.4 × 10^4 and 2.3 × 10^4

kcal^{-1}·mol·e^2 for EcDHFR and EcDHFR-N23PP/S148A, respectively) are significantly larger than those for aqueous solution (2.6 × 10^3 kcal^{-1}·mol·e^2). This is to be expected, as deforming the environment is energetically more demanding in enzymes than in solution due to the existence of a covalent structure in the proteins that does not exist in solution. As observed, the mass associated with the solvent coordinate is also significantly larger in the case of the two enzymes (1.2 × 10^{31} and 1.3 × 10^{31} kcal^{-1}·mol·e^2·s^2 for EcDHFR and EcDHFR-N23PP/S148A, respectively) than in solution (2.6 × 10^{30} kcal^{-1}·mol·e^2·s^2). The combined effect of the larger force constants and the larger associated mass for the enzymes means that the frequencies associated with the environmental motions are similar in all scenarios, and practically identical in EcDHFR and EcDHFR-N23PP/S148A (240 cm^{-1} in EcDHFR, 230 cm^{-1} in EcDHFR-N23PP/S148A, and 170 cm^{-1} in solution). Thus, environmental motions relevant for the hydride transfer have similar time scales in the three cases (of the order of picoseconds or faster). Analysis of these frequency modes reveals them to be associated with hydrogen bond pattern rearrangement around the chemical system (substrate and cofactor). The characteristic frequencies obtained for the solvent coordinate in the variant DHFR are not consistent with a mutation-induced change of the protein dynamics that could have noticeable consequences for the rate of hydride transfer. Femtosecond−picosecond time scale motions are the motions that can couple to the chemical step. This finding does however not exclude an effect from the mutations on the millisecond protein dynamics,[36] but such changes of the dynamics do not affect crossing of the barrier to hydrogen transfer.

The decrease in the rate constant observed in EcDHFR-N23PP/S148A relative to the wild type enzyme can be attributed almost exclusively to an increase in the quasi-classical activation free energy of the chemical step (Table 2). Introducing mutations into the enzyme can provoke changes in the RS and/or TS ensembles and thus in the free energy differences between them. An analysis of averaged geometries has been carried out from 2 ns QM/MM MD simulations at the TS and RS of EcDHFR and EcDHFR-N23PP/S148A. In the case of EcDHFR-N23PP/S148A, the mutations alter some protein−protein and protein−cofactor interactions established by residues belonging to the M20 loop at the reaction TS (Table S5, Supporting Information). In particular, the averaged Glu17NH···OδAsp122 distance at the TS of EcDHFR-N23PP/

S148A is 2.4 ± 0.6 Å, while this hydrogen bond interaction between the M20 and FG loops is significantly weaker in the TS of wild type EcDHFR (the averaged distance is 4.0 ± 0.7 Å). The fact that this hydrogen bond is strongly formed only in the TS of EcDHFR-N23PP/S148A could contribute to the smaller enthalpic and larger entropic barrier found experimentally for the variant.[27]

Other changes in the interactions established by the M20 loop with the cofactor or the substrate are observed upon mutation. Met20 has a reduced capability to form a S···HN hydrogen bond with the amide group of the cofactor at the TS in the variant. The averaged distances are 2.6 ± 0.3 and 3.0 ± 0.4 Å in the TSs of EcDHFR and EcDHFR-N23PP/S148A, respectively (Table S5, Supporting Information). From an electronic point of view, the formation of this hydrogen bond favors hydride transfer from the cofactor to the substrate.[51] Met20 has also been proposed to play an important role at the cofactor/substrate interface.[32] Dihedral angles of the Met20 side chain (Figure S7 and Table S5, Supporting Information) show the preference for different conformations of these residues in the wild type and variant enzymes. In support of these findings, differences in the positioning of the sulfur atom of Met20 and in the preferred conformation of its side chain between wild type EcDHFR and EcDHFR-N23PP/S148A have been observed experimentally.[36] Finally, other residues of the M20 loop such as Asn18 and Ala19 are farther from the cofactor at the TS of the variant than in wild type EcDHFR (Table S5, Supporting Information), confirming the disruption of stabilizing interactions established by this loop in the TS by mutating the enzyme.

Differences in the equilibrium fluctuations of the protein residues between wild type and variant were analyzed from the 2 ns QM/MM MD simulations of the TS by means of the root-mean-squared fluctuation (RMSF) of all residues of the proteins. The differences observed between the RMSF of residues in EcDHFR and EcDHFR-N23PP/S148A (Figure 4) are never larger than 0.5 Å in absolute value. Thus, both proteins show similar flexibility on the time scale relevant to catalysis (*vide supra*) including in the flexible βFG, βGH, and M20 loops (Figure 4A). This result is in agreement with a recent evolutionary study of DHFRs from different species, which showed that mutations do not cause large changes to the equilibrium fluctuations but that subtle changes to the equilibrium conformational sampling alter the free energy barrier of the enzymatic reaction,[52] as reflected also in our results (Table 2 and Table S5, Supporting Information). Our simulations demonstrate that residues in the active site are slightly more mobile for EcDHFR-N23PP/S148A than for the wild type enzyme in the TS (Figure 4B), reflecting the fact that protein−substrate interactions established in the active site at the TS are not as well optimized in the variant. This is consistent with a recent computational analysis of X-ray crystallographic results, which shows increased conformational heterogeneity in the active site of EcDHFR-N23PP/S148A compared to the wild type enzyme.[53]

While differences between the rate constants of EcDHFR and EcDHFR-N23PP/S148A are mostly due to changes in the equilibrium properties of the enzymes, the fact that the active site of the variant is less well set up for catalysis than the active site of the wild type also has an impact on protein motions coupled to the reaction, as previously deduced from the comparison of the recrossing transmission coefficients (Table 2). The connection between mutations and dynamics can be
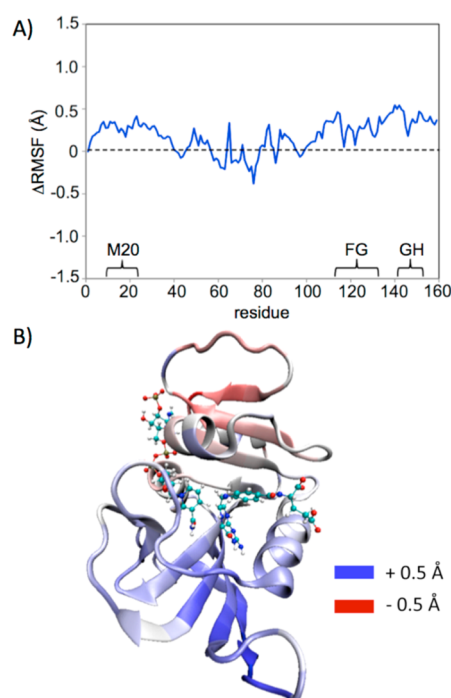

Figure 4. Differences of the femtosecond−picosecond root-mean-square fluctuations (RMSFs) between EcDHFR-N23PP/S148A and EcDHFR calculated for the backbone Cα atoms in the TSs. (A) RMSF difference versus residue number. (B) Projection on the protein backbone using a color scale: red represents regions of the protein that are more mobile in the EcDHFR than in EcDHFR-N23PP/S148A, while blue represents the opposite behavior.

rationalized observing the behavior of the environmental coordinate in the FESs (Figure 3). The ordering of the barriers without vibrational corrections is 14.6, 17.5, and 23 kcal·mol^{−1} for EcDHFR, EcDHFR-N23PP/S148A, and the reaction in aqueous solution, respectively. These values can be correlated with the displacement along the solvent coordinate s needed to reach the TS from the RS ($\Delta s^{\ddagger} = s(TS) − s(RS)$). The $\Delta s^{\ddagger}$ values obtained from the FESs for the reaction in EcDHFR, EcDHFR-N23PP/S148A, and in solution are 5, 7, and 27 kcal·mol^{−1}·e[−1], respectively. While the two enzymes stabilize the RS at a solvent coordinate closer to the value needed to reach the TS, in aqueous solution the reactants are found at a much larger value of s (∼40 kcal·mol^{−1}·e[−1]). That is, at the RS, both enzymes already provide an environment much more conducive to hydride transfer than in aqueous solution. In other words, the enzymatic active sites are preorganized to favor hydride transfer. Interestingly, the reorganization needed to reach the TS is larger for the variant than the wild type, as reflected in the larger value of $\Delta s^{\ddagger}$. Hence, the participation of protein motions in the reaction coordinate in EcDHFR-N23PP/S148A is larger than that in wild type EcDHFR. This observation agrees with the relative values of the recrossing transmission coefficients (Table 2) for the variant and the wild type that reflect a larger impact of protein motions in the former. Thus, mutations that reduce the catalytic properties of the enzymatic active site increase the participation of protein motions in the chemical step because the new active site requires a larger rearrangement to reach the TS.

CONCLUSIONS

The present investigation has used a combination of experimental and computational techniques to analyze the dynamic contributions to catalysis in EcDHFR-N23PP/S148A by comparing the heavy (^{15}N, ^{13}C, ^{2}H isotopically substituted) enzyme with its light (natural isotopic abundance) counterpart. The good agreement between the experimental and computationally derived results allows a deeper insight into the role of protein motions in enzyme catalysis. Interestingly, the impact of protein motions on catalysis is larger in EcDHFR-N23PP/S148A, previously called a "dynamic knockout" enzyme,[36] than in the wild type, as reflected in the smaller value of the recrossing transmission coefficient and the increased value of k^{LE}/k^{HE} for EcDHFR-N23PP/S148A relative to EcDHFR. Simulations that explicitly consider the changes in the environment during the chemical step show that the variant enzyme is less well set up to accommodate the chemical reaction and thus a higher degree of reorganization is required to go from the RS to the TS. This effect provokes a larger participation of protein motions in the reaction coordinate, as reflected in the smaller value of the transmission coefficient. Although millisecond conformational fluctuations in the active site of EcDHFR are lost in the N23PP/S148A variant,[36] these motions are not directly relevant to hydride transfer, as demonstrated by our characterization of the solvent coordinate changes during the chemical step. In fact, at the TS, the mobility of active site residues on the fs−ps time scale is slightly larger in EcDHFR-N23PP/S148A than in the wild type. Unlike in other enzymes, where motions on one time scale may promote those on another,[14,15] the N23PP/S148A mutation has very different effects on protein motions depending on the time scale. Motions on the μs−ms time scale are lost (at least in the M20 loop),[36] those on the ps−ns time scale are unaffected,[36] while those on the fs−ps time scale are enhanced by the mutation. EcDHFR-N23PP/S148A is therefore only a dynamic knockout on the time scale typical for conformational motions, but it is a "dynamic knock-in" at the level of the chemical step. The increased dynamic coupling of enzyme motions to the chemical coordinate is in fact detrimental to catalysis. Our findings most likely also apply to other enzyme-catalyzed reactions, although further studies are required to identify the nature of the motions that contribute to the recrossing coefficient in each case before predictive general conclusions can be drawn.

ASSOCIATED CONTENT

ⓢ Supporting Information

Experimental methods; mass spectra of purified proteins; circular dichroism spectra; tabulated experimental data for k_H, k_{cat}, K_m, and enzyme KIEs; pH dependence of k_H; computational methods; and additional computational results. This material is available free of charge via the Internet at http://pubs.acs.org.

AUTHOR INFORMATION

Corresponding Authors

ignacio.tunon@uv.es
moliner@uji.es
allemannrk@cf.ac.uk

Author Contributions

∥J.J.R.-P. and L.Y.P.L.: These authors contributed equally.

REFERENCES

(1) Warshel, A. *Proc. Natl. Acad. Sci. U.S.A.* **1984**, *81*, 444−448.

(2) Nagel, Z. D.; Klinman, J. P. *Nat. Chem. Biol.* **2009**, *5*, 543−550.

(3) Antoniou, D.; Caratzoulas, S.; Kalyanaraman, C.; Mincer, J. S.; Schwartz, S. D. *Eur. J. Biochem.* **2002**, *269*, 3103−3112.

(4) Scrutton, N. S.; Basran, J.; Sutcliffe, M. J. *Eur. J. Biochem.* **1999**, *264*, 666−671.

(5) Allemann, R. K.; Evans, R. M.; Loveridge, E. J. *Biochem. Soc. Trans.* **2009**, *37*, 349−353.

(6) Sikorski, R. S.; Wang, L.; Markham, K. A.; Rajagopalan, P. T. R.; Benkovic, S. J.; Kohen, A. *J. Am. Chem. Soc.* **2004**, *126*, 4778−4779.

(7) Wang, L.; Tharp, S.; Selzer, T.; Benkovic, S. J.; Kohen, A. *Biochemistry* **2006**, *45*, 1383−1392.

(8) Anandarajah, K.; Schowen, K. B.; Schowen, R. L. *Z. Phys. Chem.* **2008**, *222*, 1333−1347.

(9) Hay, S.; Pudney, C. R.; Scrutton, N. S. *FEBS J.* **2009**, *276*, 3930−3941.

(10) Chowdhury, S.; Banerjee, R. *J. Am. Chem. Soc.* **2000**, *122*, 5417−5418.

(11) Heyes, D. J.; Sakuma, M.; de Visser, S. P.; Scrutton, N. S. *J. Biol. Chem.* **2009**, *284*, 3762−3767.

(12) Henzler-Wildman, K.; Kern, D. *Nature* **2007**, *450*, 964−972.

(13) Frauenfelder, H.; Sligar, S. G.; Wolynes, P. G. *Science* **1991**, *254*, 1598−1603.

(14) Henzler-Wildman, K. A.; Lei, M.; Thai, V.; Kerns, S. J.; Karplus, M.; Kern, D. *Nature* **2007**, *450*, 913−916.

(15) Pineda, J. R. E. T.; Antoniou, D.; Schwartz, S. D. *J. Phys. Chem. B* **2010**, *114*, 15985−15990.

(16) Liu, H. B.; Warshel, A. *Biochemistry* **2007**, *46*, 6011−6025.

(17) Pisliakov, A. V; Cao, J.; Kamerlin, S. C. L.; Warshel, A. *Proc. Natl. Acad. Sci. U.S.A.* **2009**, *106*, 17359−17364.

(18) Glowacki, D. R.; Harvey, J. N.; Mulholland, A. J. *Nat. Chem.* **2012**, *4*, 169−176.

(19) Roca, M.; Oliva, M.; Castillo, R.; Moliner, V.; Tunon, I. *Chem.—Eur. J.* **2010**, *16*, 11399−11411.

(20) Ruiz-Pernia, J. J.; Tunon, I.; Moliner, V.; Hynes, J. T.; Roca, M. *J. Am. Chem. Soc.* **2008**, *130*, 7477−7488.

(21) Doll, K. M.; Finke, R. G. *Inorg. Chem.* **2003**, *42*, 4849−4856.

(22) Doll, K. M.; Bender, B. R.; Finke, R. G. *J. Am. Chem. Soc.* **2003**, *125*, 10877−10884.

(23) Loveridge, E. J.; Allemann, R. K. *Biochemistry* **2010**, *49*, 5390−5396.

(24) Loveridge, E. J.; Tey, L. H.; Allemann, R. K. *J. Am. Chem. Soc.* **2010**, *132*, 1137−1143.

(25) Loveridge, E. J.; Allemann, R. K. *ChemBioChem* **2011**, *12*, 1258−1262.

(26) Loveridge, E. J.; Tey, L.-H.; Behiry, E. M.; Dawson, W. M.; Evans, R. M.; Whittaker, S. B.-M.; Guenther, U. L.; Williams, C.; Crump, M. P.; Allemann, R. K. *J. Am. Chem. Soc.* **2011**, *133*, 20561−20570.

(27) Loveridge, E. J.; Behiry, E. M.; Guo, J.; Allemann, R. K. *Nat. Chem.* **2012**, *4*, 292−297.

(28) Luk, L. Y. P.; Ruiz-Pernia, J. J.; Dawson, W. M.; Roca, M.; Loveridge, E. J.; Glowacki, D. R.; Harvey, J. N.; Mulholland, A. J.; Tuñón, I.; Moliner, V.; Allemann, R. K. *Proc. Natl. Acad. Sci. U.S.A.* **2013**, *110*, 16344−16349.

(29) Benkovic, S. J.; Hammes-Schiffer, S. *Science* **2003**, *301* (80), 1196−1202.

(30) Nashine, V. C.; Hammes-Schiffer, S.; Benkovic, S. J. *Curr. Opin. Chem. Biol.* **2010**, *14*, 644−651.

(31) Liu, H. B.; Warshel, A. *J. Phys. Chem. B* **2007**, *111*, 7852−7861.

(32) Khavrutskii, I. V; Price, D. J.; Lee, J.; Brooks, C. L. *Protein Sci.* **2007**, *16*, 1087−1100.

(33) Boehr, D. D.; McElheny, D.; Dyson, H. J.; Wright, P. E. *Science* **2006**, *313*, 1638−1642.

(34) Sawaya, M. R.; Kraut, J. *Biochemistry* **1997**, *36*, 586−603.

(35) Fierke, C. A.; Johnson, K. A.; Benkovic, S. J. *Biochemistry* **1987**, *26*, 4085−4092.

(36) Bhabha, G.; Lee, J.; Ekiert, D. C.; Gam, J.; Wilson, I. A.; Dyson, H. J.; Benkovic, S. J.; Wright, P. E. *Science* **2011**, *332*, 234−238.

(37) Adamczyk, A. J.; Cao, J.; Kamerlin, S. C. L.; Warshel, A. *Proc. Natl. Acad. Sci. U.S.A.* **2011**, *108*, 14115−14120.

(38) Dametto, M.; Antoniou, D.; Schwartz, S. D. *Mol. Phys.* **2012**, *110*, 531−536.

(39) Born, M.; Oppenheimer, J. R. *Ann. Phys.* **1927**, *389*, 457−484.

(40) Kipp, D. R.; Silva, R. G.; Schramm, V. L. *J. Am. Chem. Soc.* **2011**, *133*, 19358−19361.

(41) Silva, R. G.; Murkin, A. S.; Schramm, V. L. *Proc. Natl. Acad. Sci. U.S.A.* **2011**, *108*, 18661−18665.

(42) Pudney, C. R.; Guerriero, A.; Baxter, N. J.; Johannissen, L. O.; Waltho, J. P.; Hay, S.; Scrutton, N. S. *J. Am. Chem. Soc.* **2013**, *135*, 2512−2517.

(43) Toney, M. D.; Castro, J. N.; Addington, T. A. *J. Am. Chem. Soc.* **2013**, *135*, 2509−2511.

(44) Venkitakrishnan, R. P.; Zaborowski, E.; McElheny, D.; Benkovic, S. J.; Dyson, H. J.; Wright, P. E. *Biochemistry* **2005**, *44*, 5948.

(45) Glasstone, S.; Laidler, K. J.; Eyring, H. *The theory of rate processes: the kinetics of chemical reactions, viscosity, diffusion and electrochemical phenomena*; McGraw-Hill: New York, 1941.

(46) Keck, J. C. *Adv. Chem. Phys.* **1967**, *13*, 85−121.

(47) Truhlar, D. G.; Garrett, B. C.; Klippenstein, S. J. *J. Phys. Chem.* **1996**, *100*, 12771−12800.

(48) Alhambra, C.; Corchado, J.; Sanchez, M. L.; Garcia-Viloca, M.; Gao, J.; Truhlar, D. G. *J. Phys. Chem. B* **2001**, *105*, 11326−11340.

(49) García-Meseguer, R.; Martí, S.; Ruiz-Pernía, J. J.; Moliner, V.; Tuñón, I. *Nat Chem* **2013**, *5*, 566−571.

(50) Marcus, R. A. *Annu. Rev. Phys. Chem.* **1964**, *15*, 155−196.

(51) Garcia-Viloca, M.; Truhlar, D. G.; Gao, J. *Biochemistry* **2003**, *42*, 13558−13575.

(52) Liu, C. T.; Hanoian, P.; French, J. B.; Pringle, T. H.; Hammes-Schiffer, S.; Benkovic, S. J. *Proc. Natl. Acad. Sci. U.S.A.* **2013**, *110*, 10159−10164.

(53) Van den Bedem, H.; Bhabha, G.; Yang, K.; Wright, P. E.; Fraser, J. S. *Nat. Methods* **2013**, *10*, 896−902.